Single cell transcriptomic analysis indentifies Langerhans cells immunocompetency is critical for IDO1- dependent ability to induce tolerogenic T cells.

James Davies#[1], Sofia Sirvent#[1], Andres F. Vallejo[1], Kalum Clayton[1], Gemma Porter[1], Patrick Stumpf[2], Jonathan West[3,4], Michael Ardern-Jones[1], Harinder Singh[5], Ben MacArthur[3,4], Marta E Polak[1,4]

1. Clinical and Experimental Sciences, Sir Henry Wellcome Laboratories, Faculty of Medicine, University of Southampton, SO16 6YD, Southampton, UK
2. Human Development and Health, Faculty of Medicine, University of Southampton, Southampton SO17 1BJ, UK
3. Cancer Sciences, Faculty of Medicine, University of Southampton, SO16 6YD, Southampton, UK
4. Institute for Life Sciences, University of Southampton, SO17 1BJ, UK.
5. Center for Systems Immunology, Departments of Immunology and Computational and Systems Biology, The University of Pittsburgh, Pittsburgh, PA 15213

Correspondence to:
Dr. Marta E Polak
Systems Immunology Group
Clinical and Experimental Sciences
Faculty of Medicine
University of Southampton,
SO16 6YD, Southampton, UK
e-mail: m.e.polak@soton.ac.uk
phone: +44 (0) 20815727

Abstract

Human epidermal Langerhans cells (LCs) can coordinate both immunogenic and tolerogenic immune responses, creating an attractive opportunity for immunomodulation strategies. To investigate transcriptional determinants of human primary LC tolerance we applied single cells RNA-sequencing combined with extensive functional analysis. Unsupervised clustering of single cell transcriptomes indicated that steady-state LC populations exist in a spectrum of immune activation between two states: immunocompetent and immature, distinguishable by high or low CD86 expression, respectively. Suprisingly, LC immunompetency was critical for the efficient induction of regulatory T cells during co-culture assays with naïve CD4+ T cells and expansion of autologous memory T cells. Consistently, LC tolerogenic potential was significantly enhanced upon migration from the epidermis. Transcriptional programmes underpinning LC immunocompetency, with increased expression of dendritic cell activation markers (*CD83*, *HLA-DRA* and *CCR7*), were complemented with expression of tolerogenic markers (*IDO1*, *LGALS1* and *AHR*) in migrated LC. Using protein expression analysis and perturbation with inhibitors, we confirmed the role of IDO1 as a key regulator of LC tolerogenic responses induced during LC migration, identified AHR as a potential component of IDO1-regulatory feedback loop, and demonstrated LC-mediated tolerance can be modulated through treatment with dexamethasone, indicating an opportunity for targeted therapeutic interventions in inflammatory skin disease.

Introduction

Langerhans cells (LCs) reside in the epidermis as a dense network of immune system sentinels, capable of initiating potent immune responses to cutaneous pathogens and neoplastic cells[1,2]. As a first line of the cutaneous immune defence system, LCs are uniquely specialised at sensing the environment and extend dendrites through inter-cellular tight junctions to gain access to the outermost part of the skin, the stratum corneum, so that rapid responses can be initiated if a dangerous pathogen is encountered[3]. We and others have shown that LCs are highly capable of priming and augmenting CD4 T cell responses and can induce CD8 T cell activation via antigen cross presentation more effectively than CD11c+, CD141+, CD141- and CD14+ dermal DCs[4,5,6]. However, in the context of infection, LCs can be surprisingly inefficient; LCs fail to induce cytotoxic T cell in response to herpes simplex 1 virus and in the context of *Leishmania major* infection, ablation of LCs reduced the number of activated Treg cells and aided clearance of the disease, therefore questioning the role of LC in immunogenic responses to pathogenic stimuli[7,8].

In contrast, during steady-state (non-dangerous) conditions, LCs selectively induce the activation and proliferation of skin-resident regulatory T cells[9,10] that prevent unwanted immune-mediated reactions. This key role of LCs in the maintenance of cutaneous and systemic homeostasis has been confirmed in many experimental systems. Using a mouse model for investigating LC tolerance, antigen processing and presentation of the keratinocyte protein desmoglein (Dsg3) resulted in efficient regulatory T cell (Treg) induction, whilst ablation of LCs led to increased autoimmunity[11]. LC migration from the epidermis is constantly observed during steady-state and transport of self-antigen derived from melanin to skin draining lymph nodes results in no abnormal inflammatory disease, nor does the rate of transport change

during induced inflammatory conditions[12,13,14]. In a mouse model of autoimmune encephalomyelitis, migratory skin LCs and not resident lymph DCs are required for the induction of Foxp3+ Tregs[15]. Epicutaneous delivery of OVA to OVA-sensitised mice and peanut protein to peanut-sensitised mice results in uptake and processing by skin DC and LC, but repeat exposure results in fewer inflammatory responses and an increase in Treg cells[16,17]. Similarily, LCs mediate murine tolerance during sensitisation by the hapten DNTB and is reliant on the presence of Tregs[18].

While LC-induced tolerance appears to be key to cutaneous immune homeostasis, and understanding of molecular processes underpinning this can open opportunities for targeted vaccine and immunosuppressive therapeutics, currently little is known about what biological pathways LC use for directing tolerogenic T cell immune responses. Even though some comparisons can be drawn from analysis of other tolerogenic dendritic cell subsets, LC transcriptional programming is distinct from both dendritic cells and macrophages[19,20,5,21]. Thus, in-depth analysis of human primary LCs is necessary to expand understanding of their ability to induce tolerogenic responses. Here, we used single cell RNA-seq and *in vitro* experimentation to advance understanding of LC heterogeneity and immune activation at both the steady-state and after migration, revealing important insights into how LCs mediate tolerogenic T cell responses at the epidermis.

Methods

Human LC and PBMC isolation: Human blood and skin mastectomy and abdominoplasty samples were collected with written consent from donors with approval by the South East Coast - Brighton & Sussex Research Ethics Committee in adherence to Helsinki Guidelines [ethical approvals: REC approval: 16/LO/0999). Fat

and lower dermis was cut away and discarded before dispase (2 U/ml, Gibco, UK, 20h, +4°C) digestion. For steady-state LC extraction, epidermal sheets were digested in Liberase Tm (13 U/ml, Roche, UK, 2h, +37°C,) and enriched using density gradient centrifugation (Optiprep 1:4.2, Axis Shield, Norway). Migrated LCs were extracted from epidermal explant sheets cultured in media (RPMI, Gibco, UK, 5%FBS, Invitrogen, UK, 100 IU/ml penicillin and 100 mg/ml streptomycin, Sigma, UK) for 48 hours, with or without dexamethasone (1μM, Hameln, UK). Dexamethasone stimulated migrated LC were washed with media prior to use in assays. Steady state and migrated LC were processed through fluorescence-activated cell sorting (FACS) and Drop-seq or cryopreserved in 90% FBS (Gibco, UK), 10% DMSO (Sigma, UK). PBMCs were extracted from human blood using lymphoprep (Stemcell, UK) density gradient separation. Naïve T cells were purified using the Naïve CD4+ T cell isolation kit (Miltenyi Biotec, UK). TRMs were extracted from epidermal sheets after 48 hour migration, followed by density gradient separation (Optiprep 1:3).

Flow cytometry/ FACS: Antibodies used for cell staining were pre-titrated and used at optimal concentrations. A FACS Aria flow cytometer (Becton Dickinson, USA) and DIVA software was used for analysis. For FACS purification LCs were stained for CD207 (anti-CD207 PeVio700), CD1a (anti CD1a VioBlue) and HLA-DR (anti-HLA-DR Viogreen, Miltenyi Biotech, UK). For T cell staining, antibodies anti-CD3 PerCP, anti-CD4 Viogreen, anti-CD127 Pe (Miltenyi Biotech, UK) and anti-CD25 PeCy7 (Invitrogen, UK) were used for surface staining. Anti-FOXP3 (FITC, eBiosciences, UK), anti-IL-10 (PE, Miltenyi, UK) and anti-IDO1 (AlexaFluor647, Biolegend, UK) anitbodies were used for intranuclear and intracellular staining.

Co-culture, suppression and inhibition assays: For co-culture assays, purified LC and naïve CD4+ T cells or TRMs were co-cultured in human serum supplemented media (RPMI, Gibco, UK, 10% human serum, Sigma, UK, 100 IU/ml penicillin and 100 mg/ml streptomycin, Sigma, UK) at a 1:50 ratio for 5-days at 37°C. For intranuclear FOXP3 staining T cells were permeabilised using the FOXP3/Transcription Factor Staining Buffer Set (eBiosciences, UK) following the manufacturers protocol, after cell surface marker staining. For IL-10 intracellular staining, T cells were stimulated with cell stimulation cocktail (eBioscience, UK) for 6 hours and Golgi plug (eBioscience, UK) for 5 hours, prior to intracellular staining using Permeabilizing Solution 2 (BD Biosciencies, UK). IDO1 intracellular staining of LCs was performed using Intracellular Fixation & Permeabilization Buffer Set (eBioscience, UK), following kit protocol. IDO1 inhibition experiments were performed using NLG-919 (10μM, Cambridge Bioscience UK) and epacadostat (EPAC, 1μM, Cambridge Bioscience UK) in media during migrated LC and naïve CD4+ T cell co-cultures. Proliferation assays were set up through combining FACS-purified CD3+CD4+CD127-CD25+ T cells induced after 5-day naïve CD4+ T cells and FACS-purified LC co-cultures, with autologous CFSE labelled PBMCs. PBMCs were labelled with CFSE using the CellTrace™ CFSE Cell Proliferation Kit (Invitrogen, UK), with ice cold PBS, 0.5% BSA replacing PBS and ice cold media replacing pre-warmed media as described in the protocol.

Drop-seq: After FACS purification, single LCs were co-encapsulated with primer coated barcoded Bead SeqB (Chemgenes, USA) within 1 nL droplets (Drop-seq[22]). Drop-seq microfluidic devices according to the design of Macosko *et al* were fabricated by soft lithography, oxygen plasma bonded to glass and functionalised with fluorinated silane (1% (v/v) trichloro(1H,1H,2H,2H-perfluorooctyl)silane in HFE-7500 carrier oil).

Open instrumentation syringe pumps and microscopes (see dropletkitchen.github.io) were used to generate and observe droplets, using conditions and concentrations according to the Drop-seq protocol[22], 607 steady-state LC and 208 migrated LC from mastectomy skin were converted into 'STAMPs' for PCR library amplification (High Sensitivity DNA Assay, Agilent Bioanalyser) and tagmentation (Nextera XT, Illumina, UK). Sequencing of libraries was executed using NextSeq on a paired end run (1.5x10E5 reads for maximal coverage) at the Wessex Investigational Sciences Hub laboratory, University of Southampton.

Transcriptomic data analysis: The Drop-seq protocol from the McCarrol lab[22] was followed for converting sequencer output into gene expression data. The bcl2fastq tool from Illumina was used to demultiplex files, remove UMIs from reads and deduce captured transcript reads. Reads were then aligned to human hg19 reference genome using STAR. Threshold filtering of genes with low mean counts across each cell and cells with low mean counts of all genes ensured only high-quality data was analysed. On average ~2500 genes and 85% of cells passed filtering. In an R environment, universal manifold approximation and projection (UMAP) dimensionality reduction analysis (Scater[23], singlecellTK[24]) and hierarchical clustering (clust=ward.D2, dist = canberra)[25] were used. Pseudotime trajectory analysis was performed using Slingshot (R, version 1.2.0). Differentially expressed genes (DEGs) between cell clusters were identified using Limma[26] (FDR corrected p-value<0.05, logFC>1). Gene ontology analysis was performed using Toppgene (FDR corrected p-value<0.05), describing biological pathways associated with gene lists. Public datasets from GEO used for analysis included a microarray dataset containing dexamethasone and vitamin D3 stimulated MoDC (TolMoDC) with unstimulated MoDC (GSE52894) and a microarray

dataset containing trypsinised steady-state LC with unstimulated MoDC (GSE23618) Normalised count matrices were downloaded from GEO before Limma DEG analysis. DEGs upregulated in LCs and TolMoDCs compared to unstimulated MoDCs from each respective dataset were anlaysed, with unstimulated MoDC used as reference for comparison.

Data Sharing Statement: For original data, please contact **m.e.polak@soton.ac.uk.** RNA-sequencing data are available at GEO under accession number GSE142298.

Results

Steady state LCs exist in a spectrum of immune activation from immaturity to immunocompetency.

LCs in steady-state healthy skin have been shown to expand skin resident memory Tregs which are important for mediating immune homeostasis and preventing unwarranted inflammatory responses[9]. However, when compared to dexamethasone and vitamin D3 stimulated model tolerogenic dendritic cells (TolMoDC), trypsinised steady-state LC display unique upregulated biological pathways with no crossover of differentially expressed genes (DEGs) when compared to unstimulated TolMoDC (FigureS1A, Figure S1B, Supplementary table 1A). To explore the gene expression profiles underlying healthy LC tolerogenic function and to evaluate population heterogeneity *in situ* we performed single cell RNAseq on “steady-state LC” dissociated from healthy skin using the dispase/liberase protocol, as published previously[27,28]. UMAP dimensionality reduction analysis of 607 steady-state LCs revealed heterogeneity was present amongst the population, with LCs transitioning from one state to another (Figure 1A). Using hierarchical clustering, steady-state LCs

were grouped into two defined clusters (S1 and S2) which separated the population along the transitional route (Figure 1B). Gene expression comparison after grouping genes into intervals of increasing expression level, revealed S2 LCs to be more transcriptionally active than S1 (Figure 1C). Whilst the most highly expressed genes (>10 normalised expression) in both sub populations were associated with antigen processing and presentation, the number of genes and range of expression was highest at all expression intervals in S2 LCs. Differentially expressed gene (DEG) analysis identified 21 upregulated genes (*CD74, HLA-DRA, HLA-DRB1, B2M) in* S2 LCs compared to S1 LCs, although no DEGs were identified in S1 compared to S2 (Supplementary table 2A). Whilst no specific gene ontologies were associated with tolerogenic pathways, analysis revealed associations with MHC II antigen presentation, T cell co-stimulation and response to cytokines (Figure 1D). Overall, steady-state LCs appear to exist in a spectrum of activation from lowly activated immature LC (S1) to more highly activated immunocompetent LC (S2), which likely influences their potential for coordinating T cell responses.

Steady state immunocompetent LCs are superior at inducing FOXP3+ Treg

As activation status defined LC subpopulations in the steady-state, the expression of classical DC activation markers and LC markers amongst the population was interrogated (Figure 2A, Figure S2A). Whilst *CD83* expression appeared homogenous, *CD40* was lowly detected in all steady-state LC. High HLA-DRA expression was detected in LCs from both clusters but *CD86* was predominantly expressed in S2 LC only. Following confirmation of the differential expression at the protein level using flow cytometry, CD86 was selected as a marker for distinguishing the two populations: immunocompetent and immature LCs (Figure 2B). To investigate

the immune potential of these two steady-state LC populations, CD86High and CD86Low expressing LCs were isolated using FACS (Figure 2B) and co-cultured with CD4+ naïve T cells for 5-days after which the expansion of CD25+FOXP3+ Tregs was quantified (Figure 2C, Figure S2B). Suprisingly, CD86Low immature LCs did not increase the number of CD4+CD25+FOXP3+ regulatory T cells compared to control. In contrast, CD86High immunocompetent LC significantly expanded the number of CD25+FOXP3+ Tregs compared to control (p=0.0143) and CD86Low LC (p=0.0129, n=3 independent skin donors), revealing that the state of immunocompetence associates with LC ability to promote T cell-mediated immune tolerance.

Migration enhances tolerogenic abilities of immunocompetent LCs

To explore further the link between LC activation status and tolerance induction, we sought to investigate the effect of i*n vitro* migration from epidermal sheets on LCs tolerogenic characteristics and their molecular profile. We and others have previously shown that LCs, which have migrated out of the epidermis are more immune activated and primed to mediating T cell responses[6,27,28]. Therefore, we sought to compare the capability of both steady-state LC and migrated LC to prime naïve CD4 T cells towards a tolerogenic phenotype. The expansion of CD25+FOXP3+ Tregs was measured after 5-day co-culture of naïve CD4+ T cells with LCs extracted at the steady-state via 2 hour enzymatic digestion or through migration from epidermal explants (Figure 3A). Steady-state and migrated LC both significantly amplified the percentage of CD25+FOXP3+ Tregs compared to CD4-only control (n=6 independent skin donors, steady-state LCs p=0.0101, migrated LCs p=<0.0001). However LCs ability to amplify Tregs was significantly augmented after migration, with increased percentages of CD25+FOXP3+ Tregs induced compared to steady-state LCs (Figure 3A, p=<0.0001). When co-cultured with antiCD3/CD28-stimulated PBMCs, Tregs expanded with

migratory LCs potently inhibited activated CD4 and CD8 T cell proliferation (Figure 3B, C, respectively and Figure S3A, CD4 1:1 p=0.0088, CD4 1:3 p=0.0277, CD8 1:1 p=0.0007, CD8 1:3 p=0.0111, n=5 from 3 independent LC donors). Similarily, migrated LCs efficiently expanded autologous epidermal tissue-resident memory T cells (TRMs) isolated from healthy epidermal tissue (Figure 3D, Figure S3B). Co-culture of migrated LCs with TRMs significantly increased the number of CD25+FOXP3+ Tregs compared to steady-state control (n=5 steady-state LC independent skin donors, n=4 migrated LC independent skin donors, p=0.0025). Furthermore, co-culture of migrated LCs with resident memory T cells also drove expansion of IL-10 producing CD4+ T cells, highlighting the tolerogenic capabilities of migrated LCs (Figure 3E, n=8 independent skin donors, p=0.0451).

Development of tolerogenic function is underpinned by a specific transcriptional programme.

Having confirmed the ability of highly immunocompetent migrated LCs to prime regulatory T cells, and having identified the spectrum of LC states associated with different levels of immunotolerance, allowed us to carry out analysis of transcriptional programmes and specific mediators of LC tolerogenic function. For direct comparison with steady-state LCs, 208 migrated LCs from the same donor were processed through Drop-seq for scRNA-seq. UMAP dimension reduction analysis revealed a pronounced difference in global transcriptome expression of migrated LCs, clustering separately from steady-state LCs in a single homogenous cluster (Figure 4A). Transition between the states: S1 → S2 → M was further confirmed by pseudotime trajectory analysis (Slingshot, R, version 1.2.0) Migrated LCs displayed an overall elevated expression of gene transcripts and significantly upregulated genes associated with antigen processing and presentation, cell activation and response to

cytokines (Figure 4B). Migrated LCs and steady-state LCs displayed clear differences in expression of classical DC markers and cytokines (Figure S4A). Upregulated genes in migrated LC included *CD83* and *HLA-DRA* as well as *CCR7* and *IRF4*, which have been highlighted as key regulators of LC migration and activation[27,28]. Upregulation of *CD86* was also seen in migrated LC compared to both steady-state LC clusters (Figure 4C), validating their highly immunocompetent status.

To further understand the transcriptional programmes unique to the 3 LC states, differentially expressed genes were identified in pairwise comparisons (Limma, FDR corrected p-value<0.05, LogFC>1, Supplemetary table 3A). 98 upregulated DEGs were identified comparing migrated to S1, 59 upregulated genes were identified through comparing migrated to S2. 43 upregulated DEGs were identified comparing S2 to migrated further highlighting the switch in gene expression induced after migration. Interestingly, almost all of the DEGs identified between migrated and S2 LCs were also found among the DEGs between migrated and S1 LCs (Figure S4B) suggesting that immature LCs in S1 could potentially develop immunocompetence, when stumulated. Ontology analysis (ToppGene, FDR corrected p-value<0.05) for DEGs upregulated in S2 compared to migrated included T cell receptor signalling and response to cytokine, suggesting some immune pathways were downregulated after LC migration (Figure S4C). However both migrated LC upregulated DEG lists found associations with response to cytokine, and MHC I antigen presentation, highlighting the increased activation of migrated LC compared to steady-state subsets (Figure 4D and Figure S4D). Interestingly, DEGs between migrated and S2 revealed specific associations with cell migration, regulation of dendritic cell differentiation and, importantly, T cell tolerance induction (Figure 4D). While IDO1 was expressed only in

selected steady-state cells, and was not different between S1 and S2 populations, our analysis identified differential upregulation of *LGALS1* and *AHR* in S2 (Figure 4C). LGALS1 (galectin-1) has been broadly associated with the control of a wide range of innate and adaptive immune pathways including maintenance of foetal-maternal tolerance[29,30], and AHR has been shown as an important transcription factor involved in IDO1 signalling in IDO1 signalling in DCs[31,32,33], corroborating the importance of IDO1 for LC immunotolerance.

LC-induced tolerance is mediated by IDO1 and can be enhanced by immunotherapeutic intervention.

Among all potential mediators of immunotolerance in immunocompetent LCs, *IDO1* was the most extensively expressed in migrated LC, and homogenous in this population. Consistent with the single cell RNA-seq data, the level of IDO1 protein expression was considerably and significantly higher in migrated LCs compared to steady-state LC (Figure 5A, Figure S5A, n=5 independent skin donors, p=0.0002), indicating that this molecule can be critical to migrated LC tolerogenic function. Blocking of IDO1 signalling with NLG-919, an immune checkpoint inhibitor, significantly impaired LCs ability to expand tolerogenic T cells (Figure 5B, p=0.0354). Interestingly, interference with IDO1 using epacadostat (EPAC), another selective inhibitor of tryptophan catabolism was less potent (Figure 5B, p=0.0583). LCs ability to prime and expand tolerogenic T cells creates an exciting opportunity for therapeutic interventions. Since steady-state LCs exist in a spectrum of immunocompetence, with a subpopulation of LCs already poised for tolerance induction, we hypothesised that *in situ* treatment can further potentiate their tolerogenic behaviour upon migration. To test this, we treated LCs with dexamethasone during migration from the epidermis.

Indeed, dexamethasone migrated LCs were significantly more potent in expanding CD25+FOXP3+ Tregs (Figure 5C, n=4 independent skin donors, p=0.0271) in comparison to their untreated migrated counterparts. Additionally, CD4+ T cells expanded by migratory DexLCs (n=5 independent skin donors, p=0.0061) produced more IL10 than untreated migrated LC (p=0.028), consistent with their tolerogenic phenotype (Figure 5D). Importantly, the presence of dexamethasone during LC migration further increased the expression of IDO1 protein and therefore enhanced the tolerogenic LC phenotype (n=4 independent skin donors, p=0.0142), supporting the importance of IDO1 for LC tolerogenic function (Figure 5A, Figure S5A).

Discussion

While LC-mediated immunotolerance appears critical for cutaneous and systemic immune homeostatis, research into molecular mechanisms initiating and maintaining tolerogenic behaviour in human LCs has been significantly affected by the lack of appropriate experimental models and limitations of available technologies. Here, we applied a microfluidic-based single cell and single bead co-encapsulation (Drop-seq, [22]) followed by high throughput sequencing of individual transcriptomes, to investigate transcriptional programmes in human LCs. This method allowed us to document heterogeneity in steady-state LC transcriptomes, displaying a spectrum of immune activation, previously, to the best of our knowledge, unobserved. Within this spectrum two subpopulations of steady-state LC could be identified: S1, characterised by low RNA content and immature state, and S2, which could be distinguished by high levels of CD86 expression at both mRNA and protein level, and displayed upregulated expression of antigen presenting genes, T cell co-stimulatory genes and genes generally associated with innate immune responses. Surprisingly, this latter population of LCs was characterised by ability to induce a tolerogenic T cell phenotype. Studies

have previously shown that DCs in an immature and lowly activated state, expressing low levels of antigen presenting and co-stimulatory molecules, can drive tolerogenic responses by inducing anergy of antigen-specific T cells and expanding Tregs[34,35]. However, consistent with our findings, a study by Yamazaki et al. demonstrated that mature CD86High DCs were able to expand CD4+CD25+ T cells more effectively than CD86Low immature DCs[36]. Similarly, epicutaneous immunisation of mice increased migratory LC expression of CD80 and CD86 signature markers of activation, but did not result in efficient generation of effector memory CD4 T cells[37]. Our results indicate that while low expression levels of co-stimulatory molecules on immature DC reported by others may result in impaired generation of T cell activation, induction of tolerance requires delivering of efficient signal 2 through co-stimulation. Indeed, a study of transcriptional determinant of tolerogenic and immunogenic states in murine dendrtic cells, highlighted that DC core antigen presentation module is overlayed by regulatory programmes in a tolerance-induction setting[38]. Supporting the association between immunocompetence and ability to induce tolerance, LC migration out of the epidermis resulted in an even greater ability to induce Tregs than immunocompetent (S2) steady-state LCs. Analysis of single LC transcriptomes confirmed that migratory LCs are mature and characterised by upregulation of MHC II molecules, co-stimulatory molecules (CD80 and CD86) and chemokine receptors (CCR7), indicating readiness for migration to local lymph nodes, mediating interaction with T cells to promote adaptive immune responses[39,40,41,19,27,28].

The increase in T cell co-stimulatory genes, such as CD86 and MHC class II genes in the immunocompetent S2 cluster, and in migrated LCs, suggest that physical interaction with T cells is necessary for LCs to coordinate Treg induction. Indeed, CD86 activity itself has been implicated in DC-mediated tolerance induction through

interaction with CTLA4 receptors on T cells[42,43]. However, since LC ability to induce tolerogenic responses is greatly enhanced with immunocompetence status upon migration, it is likely to be governed by additional factors complementing immune activation, the capacity to process and present antigen and interact with T cells via co-stimulatory molecules. Indeed, in parallel to LC maturation, in migrated LCs we observed expression of inducible genes previously implicated in tolerance, including *IDO1*, *LGALS1* and *AHR*. IDO1 is a classical tolerogenic mediator, which catabolises tryptophan leading to skewing of T cell differentiation towards Tregs[44]. Identified as an interferon stimulated gene (ISG), IDO1 has been previously associated with DC activation by IFNs and TNF-α[45,46] and has been implicated in a number of regulatory feedback loops in cross-talk with other cell types – e.g. activation of CTLA4 receptors on T cells in turn induces IDO1 expression in DCs[43]. Two studies in human LCs previously demonstrated induction of IDO1 steady-state LCs, and its importance for inhibition of effector T cell proliferation on stimulation with IFN-γ[47] and for FcεRI signalling[33]. Our study confirms and extends these findings, highlighting IDO1 as a key regulator of LC tolerogenic responses induced during LC migration, which is amenable to modulation, e.g. through treatment with dexamethasone, and suggests a progression of LC tolerogenic abilities from low/poised in S2, associated with transcript expression of *AHR,* to fully competent in migrated LC, mediated through high levels of IDO1 protein. Consistently, steady-state LCs, which do not express high levels of IDO1, have limited ability to activate regulatory T cells, are perhaps sufficient to maintain tolerogenic memory T cells *in situ*. In contrast, high levels of IDO1 induced by migration promote LC ability to prime naïve T cells for tolerance towards autoantigens. Sequential expression of *AHR* followed by *IDO1* upon migration provides a mechanism for inducible IDO1 expression upon activation, and suggests

the existence of a reinforcement loop for *in situ* tolerogenic responses through AHR signalling. This was previously observed in other DCs, where kynurenine metabolites, produced during IDO-mediated catabolism of tryptophan, feedback to AHRs to sustain IDO expression[31,32].

Our extensive analysis of human primary steady-state and migrated LCs indicates that while LCs with tolerogenic ability exist *in situ*, migration greatly enhances LC tolerogenic potential, likely through induction of IDO1. IDO1 dependence on pro-inflammatory and activatory signals makes it a compelling candidate as a regulator of immune activation and immune tolerance in LCs, preventing excessive activation and mediating cutaneous homeostasis. The enhancement of LC tolerogenic abilities on maturation could be explored therapeutically to reinstate tolerance in the skin during inflammatory conditions.

Acknowledgments:
We are grateful to the subjects who participated in this study. We acknowledge the use of the IRIDIS High Performance Computing Facility and Flow Cytometry Core Facilities, together with support services at the University of Southampton. The study was funded by a Sir Hendy Dale Fellowship from Wellcome Trust, 109377/Z/15/Z. Development of single cell Drop-Seq technology was funded by MRC grant MC_PC_15078.

Authorship Contributions:
MEP, SS and JD: intellectually conceived and wrote the manuscript, planned the experiments and analysed the results
SS, JD,KC,GP,AV: run functional experiments, flow cytometry, single-cell sequencing,
AV, JD, PS, JW: developed and optimisated scRNA-sequencing
JD, BMA, AV, PS, MEP: analysis and meta-analysis of scRNA-seq data
MAJ, PF, MEP, HS: discussions, data analysis, reviewing of the manuscript

Conflict of Interest Disclosures: Authors declare no conflict of interest

Figure Legends

Figure 1. Steady state LCs exist in a spectrum of immune activation from immaturity to immunocompetency

A. UMAP plot of 607 steady-state LCs (Scater, R) from 1769 genes following filtering (mitochondrial genes <0.2) and SCnorm normalisation.
B. Hierarchical clustering (clust=ward.D2, dist=canberra) of steady-state LCs defining the division of the population into two sub clusters, steady-state 1 (S1) and steady-state 2 (S2).
C. S1 and S2 normalised gene expression values were grouped into expression level intervals (y-axis). The number of genes included in each interval and the top associated biological processes identified using ToppGene gene ontology analysis are displayed with significance values (FDR corrected p-value).
D. Gene ontology analysis using ToppGene of 21 DEGs upregulated in S2 LC compared to S1 LC. -log(10) FDR corrected FDR corrected p-values are displayed.

Figure 2. Steady state immunocompetent LCs are superior at inducing FOXP3+ Tregs

A. UMAP markers plots displaying *CD86, CD83*, *HLA-DRA* and *CD40* expression amongst the steady-state LC population displaying low (grey) to high (dark red) SCnorm normalised expression.
B. Flow cytometry assessment of steady-state LCs identified as CD207/CD1a high cells. LC populations were separated into CD86Low and CD86High by FACS. Representative example from n=3 independentLC donors.
C. Flow cytometry assessment of CD4+ naive T cells after 5-day co-culture with either CD86Low or CD86High steady-state LC. 5-day cultures of CD4+ naïve T cells alone were used as control. Tregs were identified as CD3+CD4+CD127-CD25+FOXP3+ cells. n=3 independent LC donor paired experiments. *p<0.05.

Figure 3. Migration enhances tolerogenic abilities of immunocompetent LCs

A. Flow cytometry assessment of the percentage of Tregs induced after 5-day co-culture of steady-state LC and migrated LC with CD4+ naive T cells. 5-day cultures of CD4+ naïve T cells alone were used as control. Tregs were identified as CD3+CD4+CD127-CD25+FOXP3+ cells. n=8 control, 5 steady-state and 6 migrated independent LC donors. *p<0.05, **p<0.01, ***p<0.001.
B. CFSE labelled PBMCs gated on CD4+ T cells proliferation measurements after 3-day co-culture with autologous purified CD3+CD4+CD127-CD25+ Tregs. The percentage of proliferating CD4+ cells stimulated with plate bound anti-CD3 and soluble anti-CD28 is displayed at ratios of 1:1 and 1:3 Treg:PBMC (n=5 from 3 independent LC donors). *p<0.05, **p<0.01.
C. CFSE labelled PBMCs, gated on CD8+ T cells, proliferation measurements after 3-day co-culture with autologous purified CD3+CD4+CD127-CD25+ Tregs. The percentage of proliferating CD8+ cells stimulated with plate bound anti-CD3 and soluble anti-CD28 is displayed at ratios of 1:1 and 1:3 Treg:PBMC (n=5 from 3 independent LC donors). *p<0.05, ***p<0.001.
D. Flow cytometry assessment of the percentage of Tregs induced after 5-day co-culture of migrated LC with autologous T resident memory cells (TRMs) extracted from human epidermis. 5-day cultures of TRMs alone were used as

control. Tregs were identified as CD3+CD4+CD127-CD25+FOXP3+ cells. n=5 independent LC donors. **p<0.01.

E. Percentage of IL-10 producing CD4+ cells after co-culture of TRMs with or without migrated LC. n=8. *p<0.05.

Figure 4. Development of tolerogenic function is underpinned by a specific transcriptomic programme.

A. UMAP plot of 607 steady-state LCs (Figure 1a) and 208 migrated LCs (Scater, R) from 3363 genes following filtering (mitochondrial genes <0.2) and SCnorm normalisation.
B. Migrated LC normalised gene expression values were grouped into expression intervals (y-axis). The number of genes included in each interval and the top associated biological processes identified using ToppGene gene ontology analysis are displayed with significance values (FDR corrected Benjamini-Hochberg).
C. UMAP markers plots displaying CD86 and the tolerogenic markers *IDO1, LGALS1* and *AHR* expression amongst the steady-state and migrated LC, displaying low (grey) to high (dark red) expression.
D. Gene ontology analysis using ToppGene of 59 DEGs upregulated in M LC compared to immunocompetent S2 LC. -log(10) FDR corrected p-values are displayed.

Figure 5. LC-induced tolerance is mediated by IDO1 and can be enhanced by immunotherapeutic intervention.

A. Flow cytometry assessment of the percentage of IDO1 expression in steady-state LC and migrated LC extracted by 48 hour culture of epidermal sheets with and without 1M dexamethasone. n=5 steady-state and migrated independent LCs, n=4 migrated dexamethasone independent LCs. *p<0.05, ***p<0.001, ****p<0.0001.
B. Flow cytometry analysis of the percentage of Tregs induced after 5-day co-culture of migrated LC with CD4+ naïve T cells in the presence of IDO1 inhibitors NLG-919 (NLG) and epacadostat (EPAC). 5-day cultures of CD4+ naïve T cells alone were used as control. Tregs were identified as CD3+CD4+CD127-CD25+FOXP3+ cells. n=4 independent LC donors. *p<0.05.
C. Flow cytometry assessment of the percentage of Tregs induced after 5-day co-culture of migrated LC with and without dexamethasone stimulation, with CD4+ naive T cells. Tregs were identified as CD3+CD4+CD127-CD25+FOXP3+ cells. n=4 independent LC donors. *p<0.05.
D. Flow cytometry analysis of the percentage of CD4+IL10+ T cells after 5-day co-culture of migrated LC with and without dexamethasone stimulation, with CD4+ naïve T cells. 5-day cultures of CD4+ naïve T cells alone were used as control. n=5 independent LC donors. *p<0.05, **p<0.01.

Figure S1. Steady state LCs exist in a spectrum of immune activation from immaturity to immunocompetency

A. Biological pathways identified from gene ontology analysis (ToppGene) of 86s DEGs upregulated in trypsinised steady-state LC compared unstimulated MoDC (GSE23618) and 171 DEGs upregulated in Dexamethasone and

Vitamin D3 treated MoDC (TolMoDC) compared to unstimulated MoDC (GSE52894) identified using Limma (FDR corrected p-value<0.05, logFC>1). -log(10) FDR corrected p-values are displayed.

B. Venn diagram displaying crossover between upregulated DEGs identified comparing in trypsinised steady-state LC to unstimulated MoDC (GSE23618), and TolMoDC to unstimulated MoDC (GSE52894).

Figure S2. Steady state immunocompetent LCs are superior at inducing FOXP3+ Tregs

A. UMAP markers plots displaying *CD207* and *IL1B* expression amongst the steady-state LC population displaying low (grey) to high (dark red) SCnorm normalised expression.
B. Gating strategy for investigating the quantity of CD3+CD4+CD127-CD25+FOXP3+ Tregs after co-culture of CD4 naïve T cells with LC for 5-days.

Figure S3. Migration enhances tolerogenic abilities of immunocompetent LCs

A. Gating strategy for investigating CFSE labelled PBMC proliferation, selecting for CD4+ and CD8+ T cell populations. CFSE measurement gating was applied to responder cell population only, excluding unlabelled CFSE negative Tregs.
B. Gating strategy for investigating the quantity of Tregs induced after co-culture of autologous TRMs with migrated LC for 5-days.

Figure S4. Development of tolerogenic function is underpinned by a specific transcriptional programme.

A. UMAP markers plots displaying *HLA-DRA, HLA-B, B2M, CCL22, CCR7, CD83, IRF4, CD207* and *IL8* expression amongst the steady-state and migrated LC population displaying low (grey) to high (dark red) SCnorm normalised expression.
B. Venn diagram displaying the overlap in DEGs upregulated in migrated (M) compared to steady-state 1 (S1) or steady-state 2 (S2) LC (Limma, FDR corrected p-value<0.05, logFC>1).
C. Gene ontology analysis using ToppGene of 43 DEGs upregulated in steady-state 2 (S2) LC compared to migrated (M) LC. -log(10) FDR corrected p-values are displayed.
D. Gene ontology analysis using ToppGene of 98 DEGs upregulated in migrated (M) LC compared to steady-state 1 (S1) LC. -log(10) FDR corrected p-values are displayed.

Figure S5. LC-induced tolerance is mediated by IDO1 can be enhanced by immunotherapeutic intervention.

A. Gating strategy to define the percentage of IDO1 expression in steady-state LC, migrated, and dexamethasone migrated LC. n=5 steady-state and migrated LC experiments, n=4 migrated dexamethasone experiments.

Supplementary Table 1. Trypsinised steady-state LC and TolMoDC DEGs

A. DEGs comparing trypsined steady-state LC to unstimulated MoDC (GSE23618) and TolMoDC to unstimulated MoDC (GSE52894) were indentified using Limma (FDR corrected p-value<0.05, logFC>1). Biological pathways associated with DEGs were identified in Toppgene (FDR corrected p-value<0.05).

Supplementary Table 2. Steady state LC DEG analysis

A. DEGs comparing steady-state S1 and S2 LC using Limma (FDR corrected p-value<0.05, logFC>1). Biological pathways associated with DEGs were identified in Toppgene (FDR corrected p-value<0.05).

Supplementary Table 3. Migrated and Steady state LC DEG analysis

A. DEGs comparing migrated, steady-state S1 and S2 LC using Limma (FDR corrected p-value<0.05, logFC>1). Biological pathways associated with DEGs were identified in Toppgene (FDR corrected p-value<0.05).

References

1. Mutyambizi, K., Berger, C. L. & Edelson, R. L. The balance between immunity and tolerance: the role of Langerhans cells. *Cell. Mol. Life Sci.* **66**, 831–40 (2009).
2. Deckers, J., Hammad, H. & Hoste, E. Langerhans Cells: Sensing the Environment in Health and Disease. *Front. Immunol.* **9**, 93 (2018).
3. Kubo, A., Nagao, K., Yokouchi, M., Sasaki, H. & Amagai, M. External antigen uptake by Langerhans cells with reorganization of epidermal tight junction barriers. *J. Exp. Med.* **206**, 2937–2946 (2009).
4. Polak, M. E. *et al.* CD70-CD27 interaction augments CD8+ T-cell activation by human epidermal Langerhans cells. *J. Invest. Dermatol.* **132**, 1636–44 (2012).
5. Artyomov, M. N. *et al.* Modular expression analysis reveals functional conservation between human Langerhans cells and mouse cross-priming dendritic cells. *J. Exp. Med.* **212**, 743–57 (2015).
6. Klechevsky, E. *et al.* Functional specializations of human epidermal Langerhans cells and CD14+ dermal dendritic cells. *Immunity* **29**, 497–510 (2008).
7. Allan, R. S. *et al.* Epidermal viral immunity induced by CD8alpha+ dendritic cells but not by Langerhans cells. *Science* **301**, 1925–8 (2003).
8. Ritter, U., Meißner, A., Scheidig, C. & Körner, H. CD8α- and Langerin-negative dendritic cells, but not Langerhans cells, act as principal antigen-presenting cells in leishmaniasis. *Eur. J. Immunol.* **34**, 1542–1550 (2004).
9. Seneschal, J. *et al.* Human Epidermal Langerhans Cells Maintain Immune Homeostasis in Skin by Activating Skin Resident Regulatory T Cells. *Immunity* **36**, 873–884 (2012).
10. van der Aar, A. M. G. *et al.* Langerhans Cells Favor Skin Flora Tolerance through Limited Presentation of Bacterial Antigens and Induction of Regulatory T Cells. *J. Invest. Dermatol.* **133**, 1240–1249 (2013).
11. Kitashima, D. Y. *et al.* Langerhans Cells Prevent Autoimmunity via Expansion of Keratinocyte Antigen-Specific Regulatory T Cells. *EBioMedicine* **27**, 293–303 (2018).
12. Ghigo, C. *et al.* Multicolor fate mapping of Langerhans cell homeostasis. *J. Exp. Med.* **210**, 1657–64 (2013).
13. Hemmi, H. *et al.* Skin antigens in the steady state are trafficked to regional lymph nodes by transforming growth factor-β1-dependent cells. *Int. Immunol.* **13**, 695–704 (2001).

14. Yoshino, M., Yamazaki, H., Shultz, L. D. & Hayashi, S.-I. Constant rate of steady-state self-antigen trafficking from skin to regional lymph nodes. *Int. Immunol.* **18**, 1541–1548 (2006).
15. Idoyaga, J. *et al.* Specialized role of migratory dendritic cells in peripheral tolerance induction. *J. Clin. Invest.* **123**, 844–54 (2013).
16. Dioszeghy, V. *et al.* Epicutaneous Immunotherapy Results in Rapid Allergen Uptake by Dendritic Cells through Intact Skin and Downregulates the Allergen-Specific Response in Sensitized Mice. *J. Immunol.* **186**, 5629–5637 (2011).
17. Dioszeghy, V. *et al.* Differences in phenotype, homing properties and suppressive activities of regulatory T cells induced by epicutaneous, oral or sublingual immunotherapy in mice sensitized to peanut. *Cell. Mol. Immunol.* **14**, 770–782 (2017).
18. Gomez de Agüero, M. *et al.* Langerhans cells protect from allergic contact dermatitis in mice by tolerizing CD8(+) T cells and activating Foxp3(+) regulatory T cells. *J. Clin. Invest.* **122**, 1700–11 (2012).
19. Polak, M. E. *et al.* Distinct Molecular Signature of Human Skin Langerhans Cells Denotes Critical Differences in Cutaneous Dendritic Cell Immune Regulation. *J. Invest. Dermatol.* **134**, 695–703 (2014).
20. Clayton, K., Vallejo, A. F., Davies, J., Sirvent, S. & Polak, M. E. Langerhans Cells—Programmed by the Epidermis. *Front. Immunol.* **8**, 1676 (2017).
21. Duluc, D. *et al. Transcriptional fingerprints of antigen-presenting cell subsets in the human vaginal mucosa and skin reflect tissue-specific immune microenvironments*. (2014). doi:10.1186/s13073-014-0098-y
22. Macosko, E. Z. *et al.* Highly Parallel Genome-wide Expression Profiling of Individual Cells Using Nanoliter Droplets. *Cell* **161**, 1202–1214 (2015).
23. McCarthy, D. J., Campbell, K. R., Lun, A. T. L. & Wills, Q. F. Scater: pre-processing, quality control, normalization and visualization of single-cell RNA-seq data in R. *Bioinformatics* **347**, btw777 (2017).
24. Jenkins, D., Faits, T., Khan, M., Carrasco Pro, S. & Johnson, W. singleCellTK: Interactive Analysis of Single Cell RNA-Seq Data. (2018).
25. Satija, R., Farrell, J. A., Gennert, D., Schier, A. F. & Regev, A. Spatial reconstruction of single-cell gene expression data. *Nat. Biotechnol.* **33**, 495–502 (2015).
26. Ritchie, M. E. *et al.* limma powers differential expression analyses for RNA-sequencing and microarray studies. *Nucleic Acids Res.* **43**, e47–e47 (2015).
27. Polak, M. *et al.* Genomic programming of antigen cross-presentation in IRF4-expressing human Langerhans cells. *bioRxiv* (2019). doi:10.1101/541383
28. Sirvent, S. *et al.* Genomic programming of IRF4-expressing human Langerhans cells. *Nat. Commun.* **Pre-print**, (2019).
29. Sundblad, V., Morosi, L. G., Geffner, J. R. & Rabinovich, G. A. Galectin-1: A Jack-of-All-Trades in the Resolution of Acute and Chronic Inflammation. *J. Immunol.* **199**, 3721–3730 (2017).
30. Blois, S. M. *et al.* A pivotal role for galectin-1 in fetomaternal tolerance. *Nat. Med.* **13**, 1450–1457 (2007).
31. Li, Q., Harden, J. L., Anderson, C. D. & Egilmez, N. K. Tolerogenic Phenotype of IFN-γ-Induced IDO+ Dendritic Cells Is Maintained via an Autocrine IDO-Kynurenine/AhR-IDO Loop. *J. Immunol.* **197**, 962–70 (2016).
32. Nguyen, N. T. *et al.* Aryl hydrocarbon receptor negatively regulates dendritic cell immunogenicity via a kynurenine-dependent mechanism. *Proc. Natl. Acad. Sci.* **107**, 19961–19966 (2010).

33. Koch, S. *et al.* AhR mediates an anti-inflammatory feedback mechanism in human Langerhans cells involving FcεRI and IDO. *Allergy* **72**, 1686–1693 (2017).
34. Mahnke, K., Schmitt, E., Bonifaz, L., Enk, A. H. & Jonuleit, H. Immature, but not inactive: the tolerogenic function of immature dendritic cells. *Immunol. Cell Biol.* **80**, 477–483 (2002).
35. Hasegawa, H. & Matsumoto, T. Mechanisms of Tolerance Induction by Dendritic Cells In Vivo. *Front. Immunol.* **9**, 350 (2018).
36. Yamazaki, S. *et al.* Direct Expansion of Functional CD25 CD4 Regulatory T Cells by Antigen-processing Dendritic Cells. *J. Exp. Med. J. Exp. Med.* □ **198**, 235–247 (2003).
37. Shklovskaya, E. *et al.* Langerhans cells are precommitted to immune tolerance induction. *Proc. Natl. Acad. Sci. U. S. A.* **108**, 18049–54 (2011).
38. Vander Lugt, B. *et al.* Transcriptional determinants of tolerogenic and immunogenic states during dendritic cell maturation. *J. Cell Biol.* **216**, 779–792 (2017).
39. Shklovskaya, E., Roediger, B. & Fazekas de St Groth, B. Epidermal and dermal dendritic cells display differential activation and migratory behavior while sharing the ability to stimulate CD4+ T cell proliferation in vivo. *J. Immunol.* **181**, 418–30 (2008).
40. Villablanca, E. J. & Mora, J. R. A two-step model for Langerhans cell migration to skin-draining LN. *Eur. J. Immunol.* **38**, 2975–2980 (2008).
41. Cumberbatch, M., Dearman, R. J., Griffiths, C. E. M. & Kimber, I. Langerhans cell migration. Experimental dermatology . Review article. *Clin. Exp. Dermatol.* **25**, 413–418 (2000).
42. Mellor, A. L. *et al.* Specific subsets of murine dendritic cells acquire potent T cell regulatory functions following CTLA4-mediated induction of indoleamine 2,3 dioxygenase. *Int. Immunol.* **16**, 1391–1401 (2004).
43. Obregon, C., Kumar, R., Pascual, M. A., Vassalli, G. & Golshayan, D. Update on Dendritic Cell-Induced Immunological and Clinical Tolerance. *Front. Immunol.* **8**, 1514 (2017).
44. Curti, A., Trabanelli, S., Salvestrini, V., Baccarani, M. & Lemoli, R. M. The role of indoleamine 2,3-dioxygenase in the induction of immune tolerance: focus on hematology. *Blood* **113**, 2394–2401 (2009).
45. Mellor, A. L., Lemos, H. & Huang, L. Indoleamine 2,3-Dioxygenase and Tolerance: Where Are We Now? *Front. Immunol.* **8**, 1360 (2017).
46. Braun, D., Longman, R. S. & Albert, M. L. A two-step induction of indoleamine 2,3 dioxygenase (IDO) activity during dendritic-cell maturation. *Blood* **106**, 2375–2381 (2005).
47. von Bubnoff, D. *et al.* Human Epidermal Langerhans Cells Express the Immunoregulatory Enzyme Indoleamine 2,3-Dioxygenase. *J. Invest. Dermatol.* **123**, 298–304 (2004).

Figure 1

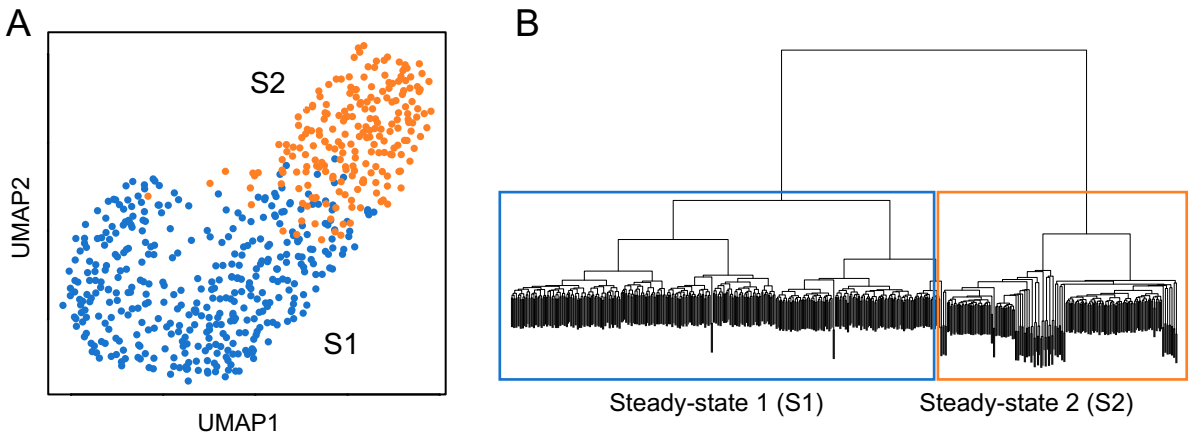
A
S2
S1
UMAP2
UMAP1
B
Steady-state 1 (S1)
Steady-state 2 (S2)

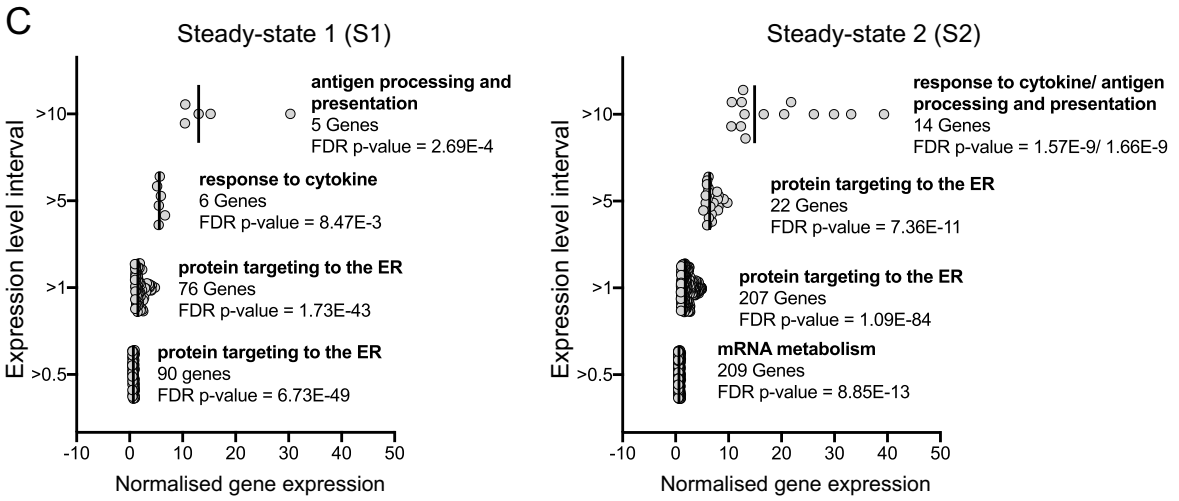
C
Steady-state 1 (S1)
antigen processing and presentation
5 Genes
FDR p-value = 2.69E-4
response to cytokine
6 Genes
FDR p-value = 8.47E-3
protein targeting to the ER
76 Genes
FDR p-value = 1.73E-43
protein targeting to the ER
90 genes
FDR p-value = 6.73E-49
Expression level interval
>10
>5
>1
>0.5
-10 0 10 20 30 40 50
Normalised gene expression
Steady-state 2 (S2)
response to cytokine/ antigen processing and presentation
14 Genes
FDR p-value = 1.57E-9/ 1.66E-9
protein targeting to the ER
22 Genes
FDR p-value = 7.36E-11
protein targeting to the ER
207 Genes
FDR p-value = 1.09E-84
mRNA metabolism
209 Genes
FDR p-value = 8.85E-13
Expression level interval
>10
>5
>1
>0.5
-10 0 10 20 30 40 50
Normalised gene expression

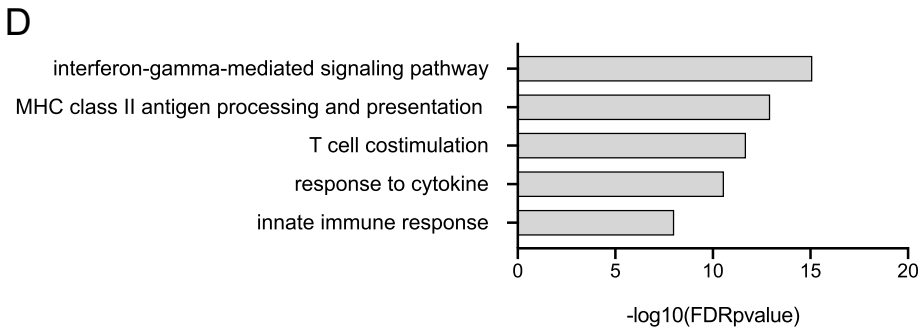
D
interferon-gamma-mediated signaling pathway
MHC class II antigen processing and presentation
T cell costimulation
response to cytokine
innate immune response
0 5 10 15 20
-log10(FDRpvalue)

Figure 2

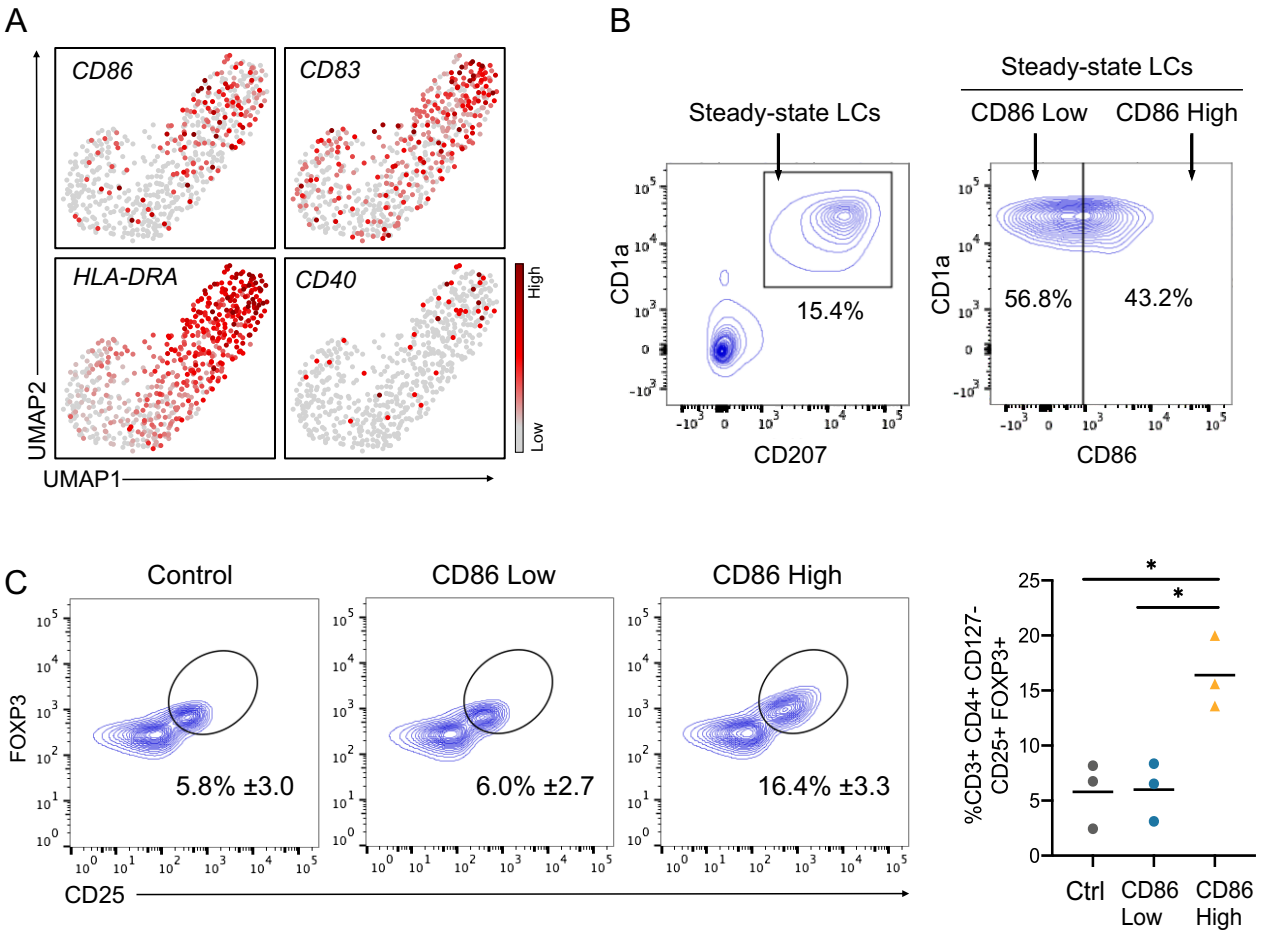
A
CD86
CD83
HLA-DRA
CD40
High
Low
UMAP2
UMAP1
B
Steady-state LCs
CD1a
15.4%
CD207
Steady-state LCs
CD86 Low
CD86 High
CD1a
56.8%
43.2%
CD86
C
Control
CD86 Low
CD86 High
FOXP3
5.8% ±3.0
6.0% ±2.7
16.4% ±3.3
CD25
%CD3+ CD4+ CD127- CD25+ FOXP3+
Ctrl
CD86 Low
CD86 High

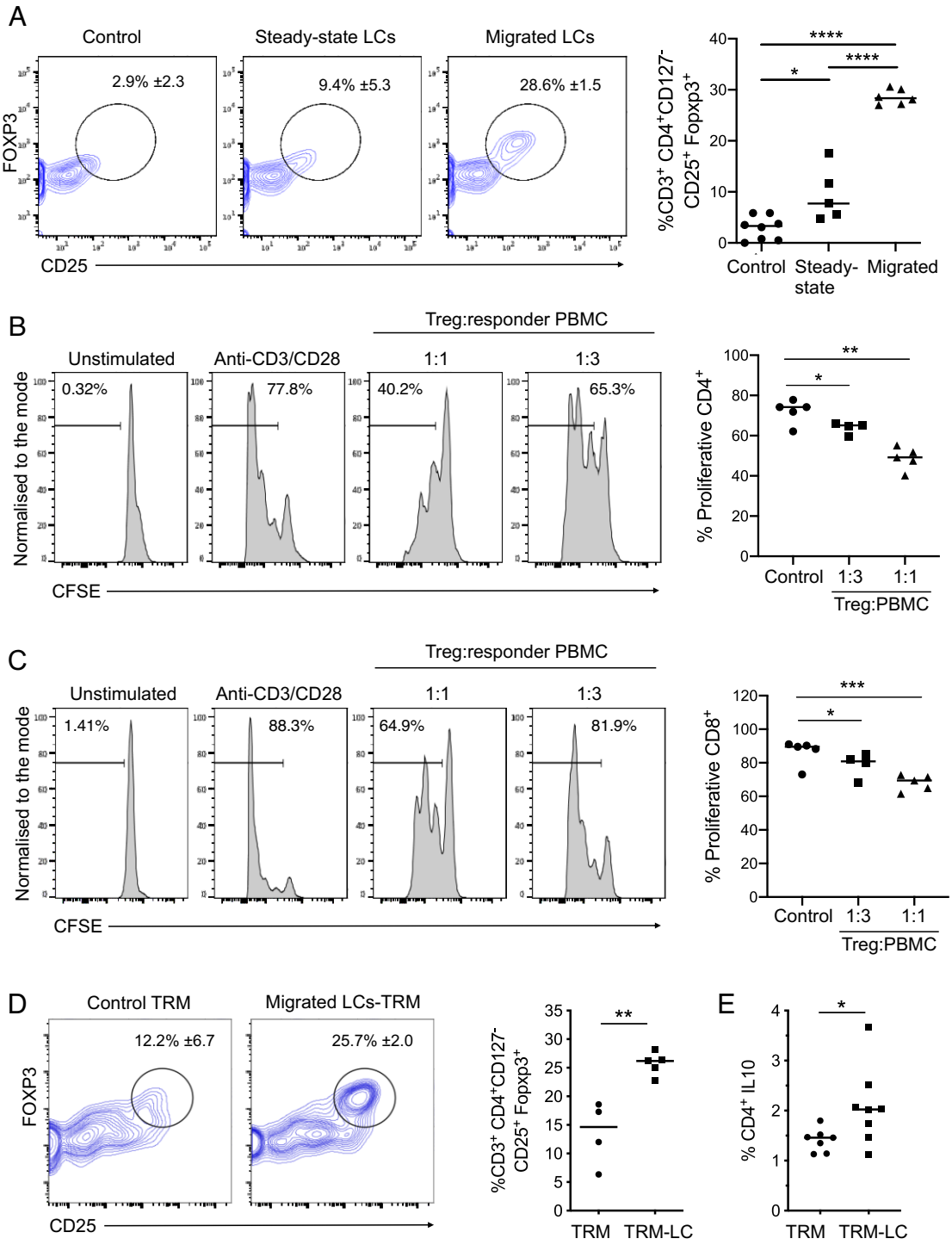
A
Control
Steady-state LCs
Migrated LCs
2.9% ±2.3
9.4% ±5.3
28.6% ±1.5
FOXP3
CD25
%CD3+ CD4+CD127- CD25+ Foxp3+
Control
Steady-state
Migrated
B
Treg:responder PBMC
Unstimulated
Anti-CD3/CD28
1:1
1:3
0.32%
77.8%
40.2%
65.3%
Normalised to the mode
CFSE
% Proliferative CD4+
Control
1:3
1:1
Treg:PBMC
C
Treg:responder PBMC
Unstimulated
Anti-CD3/CD28
1:1
1:3
1.41%
88.3%
64.9%
81.9%
Normalised to the mode
CFSE
% Proliferative CD8+
Control
1:3
1:1
Treg:PBMC
D
Control TRM
Migrated LCs-TRM
12.2% ±6.7
25.7% ±2.0
FOXP3
CD25
%CD3+ CD4+CD127- CD25+ Foxp3+
TRM
TRM-LC
E
% CD4+ IL10
TRM
TRM-LC

Figure 4

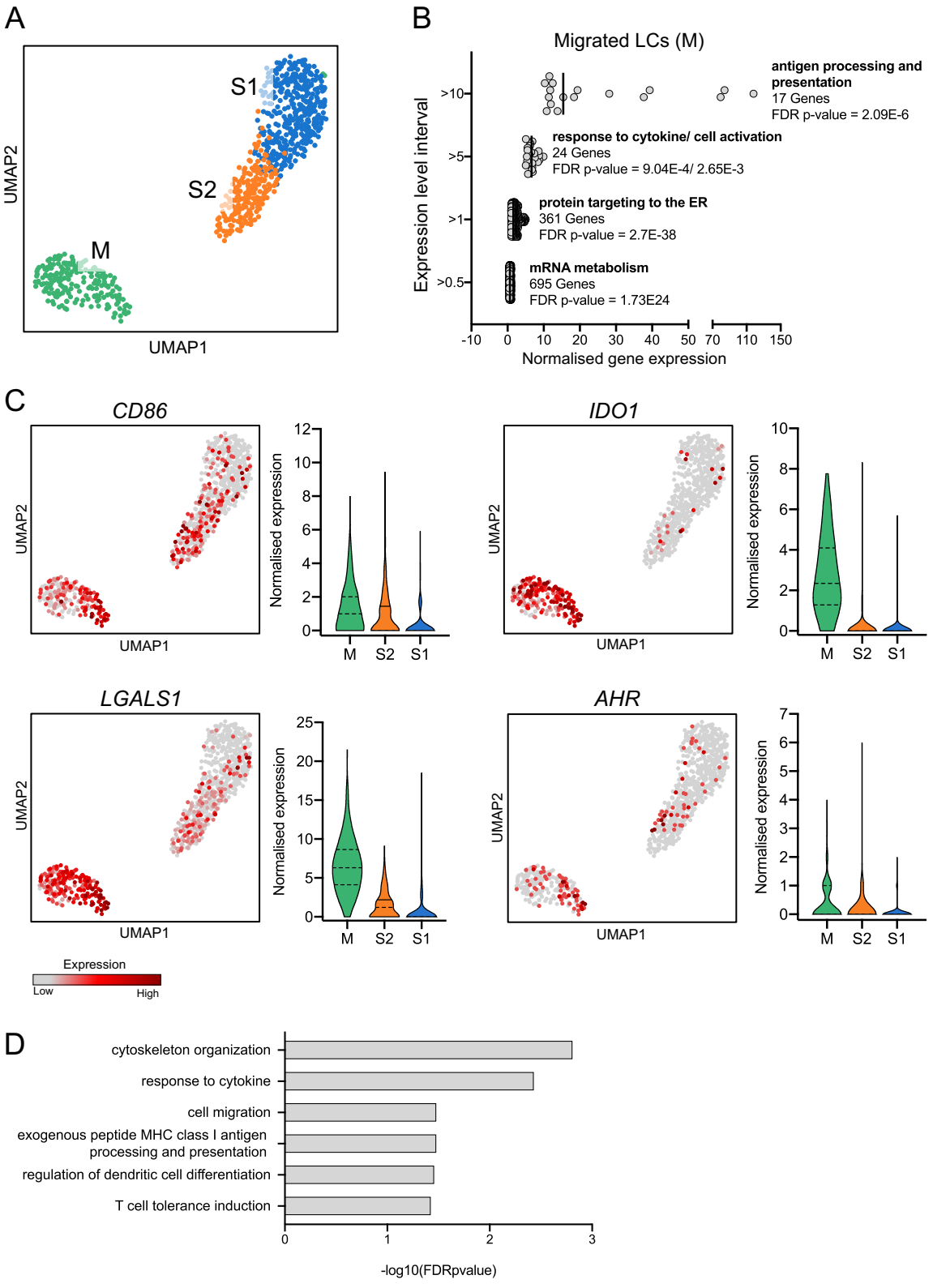
A
S1
S2
M
UMAP2
UMAP1
B
Migrated LCs (M)
Expression level interval
>10
>5
>1
>0.5
antigen processing and presentation
17 Genes
FDR p-value = 2.09E-6
response to cytokine/ cell activation
24 Genes
FDR p-value = 9.04E-4/ 2.65E-3
protein targeting to the ER
361 Genes
FDR p-value = 2.7E-38
mRNA metabolism
695 Genes
FDR p-value = 1.73E24
-10 0 10 20 30 40 50 70 110 150
Normalised gene expression
C
CD86
IDO1
LGALS1
AHR
UMAP2
UMAP1
Normalised expression
M S2 S1
Expression
Low
High
D
cytoskeleton organization
response to cytokine
cell migration
exogenous peptide MHC class I antigen processing and presentation
regulation of dendritic cell differentiation
T cell tolerance induction
0 1 2 3
-log10(FDRpvalue)

Figure 5

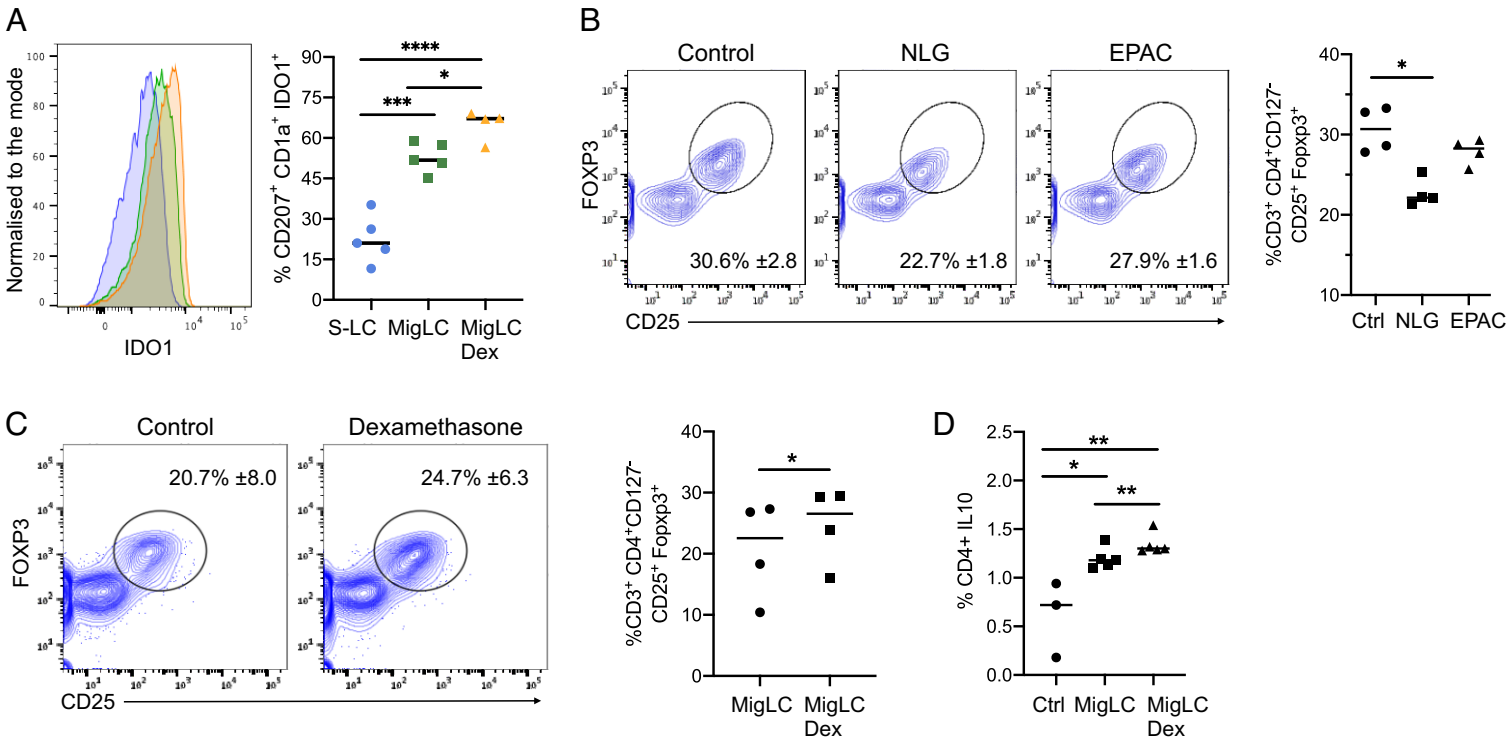
A
Normalised to the mode
IDO1
% CD207+ CD1a+ IDO1+
S-LC
MigLC
MigLC Dex
B
Control
NLG
EPAC
FOXP3
CD25
30.6% ±2.8
22.7% ±1.8
27.9% ±1.6
%CD3+ CD4+CD127- CD25+ Fopxp3+
Ctrl
NLG
EPAC
C
Control
Dexamethasone
20.7% ±8.0
24.7% ±6.3
FOXP3
CD25
%CD3+ CD4+CD127- CD25+ Fopxp3+
MigLC
MigLC Dex
D
% CD4+ IL10
Ctrl
MigLC
MigLC Dex

Supplementary Figure 1

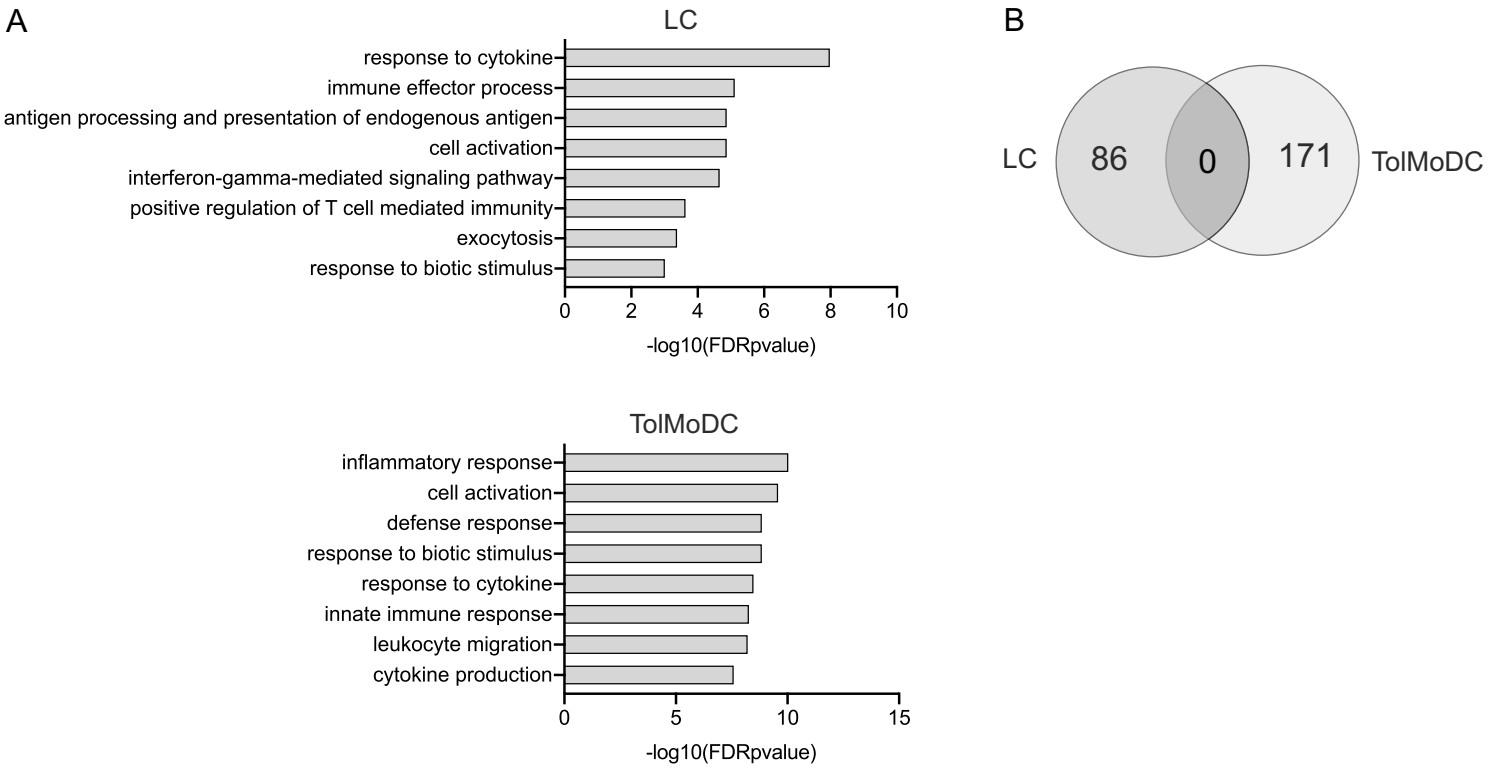

Supplementary Figure 2

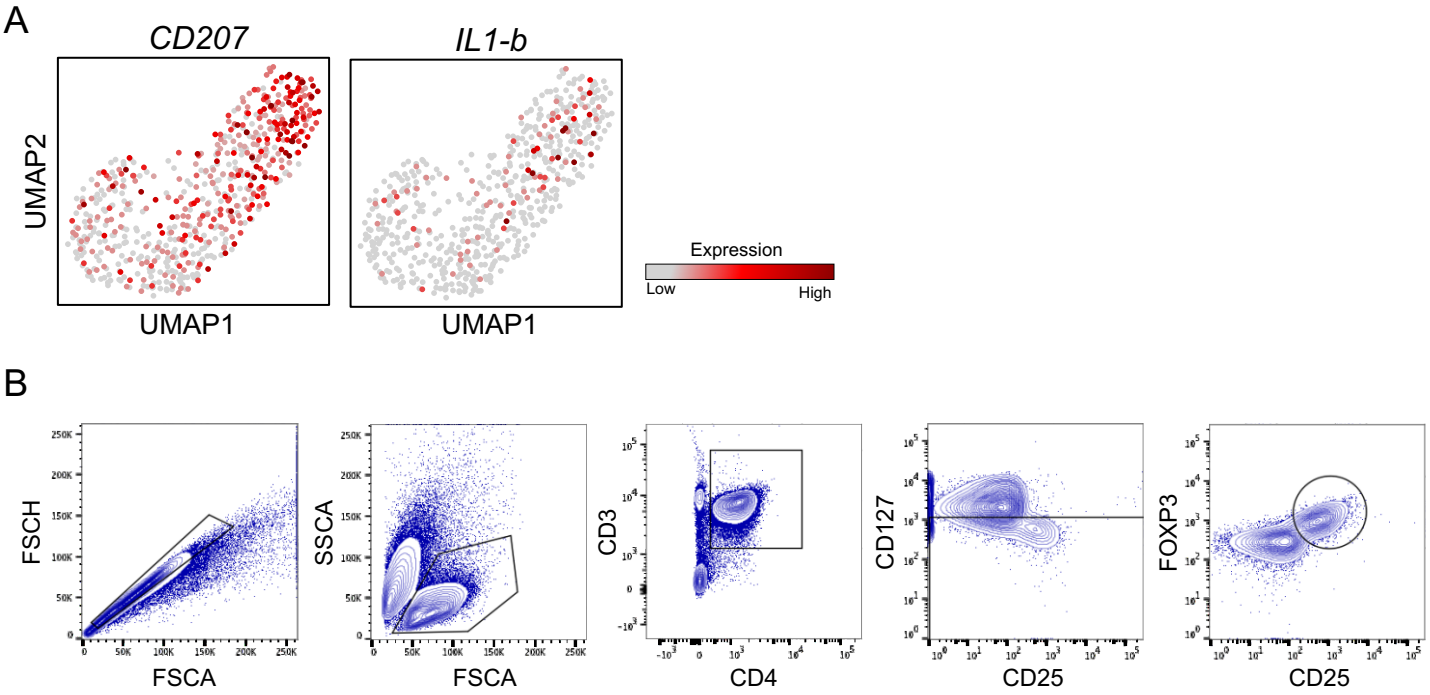

Supplementary Figure 3

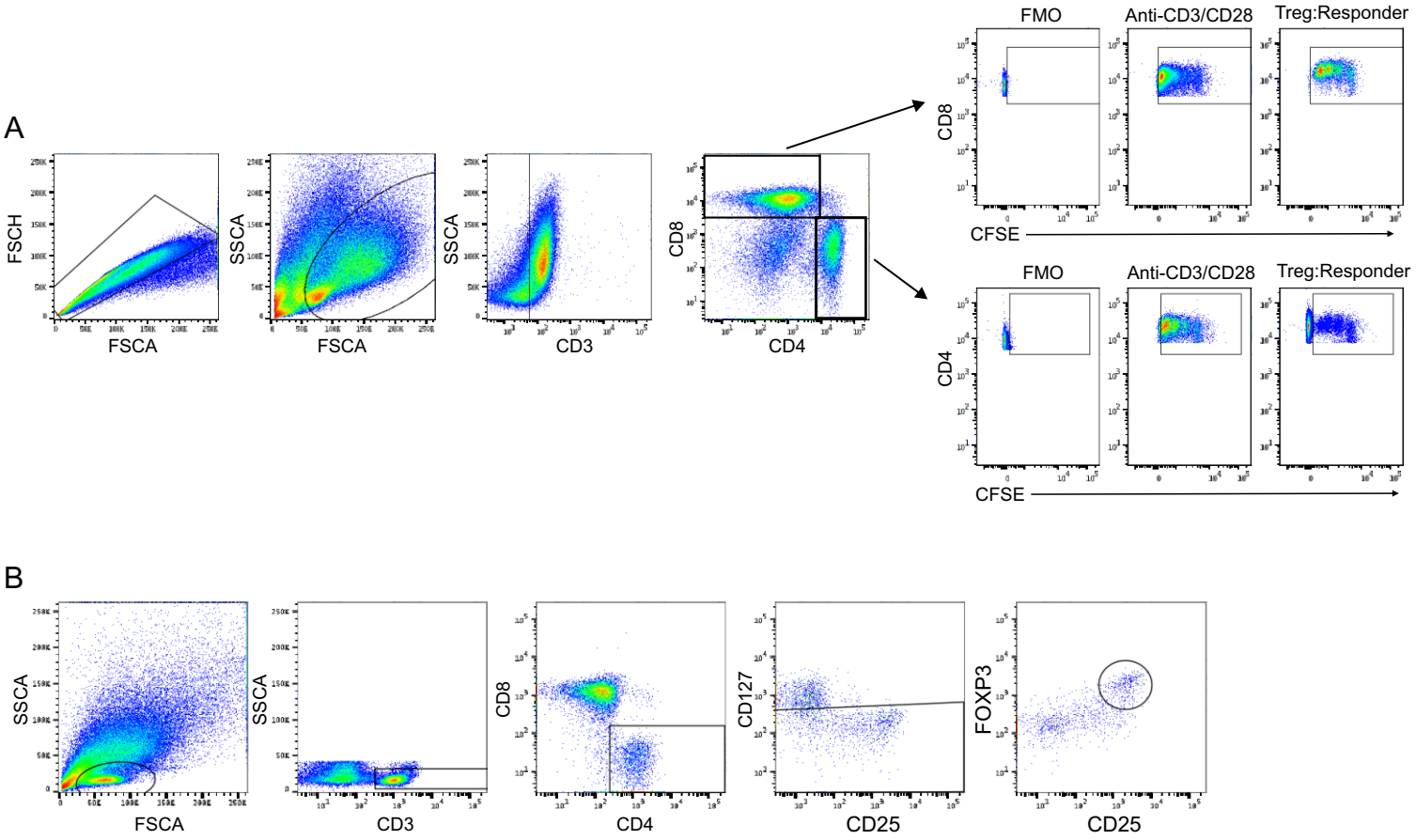

Supplementary Figure 4

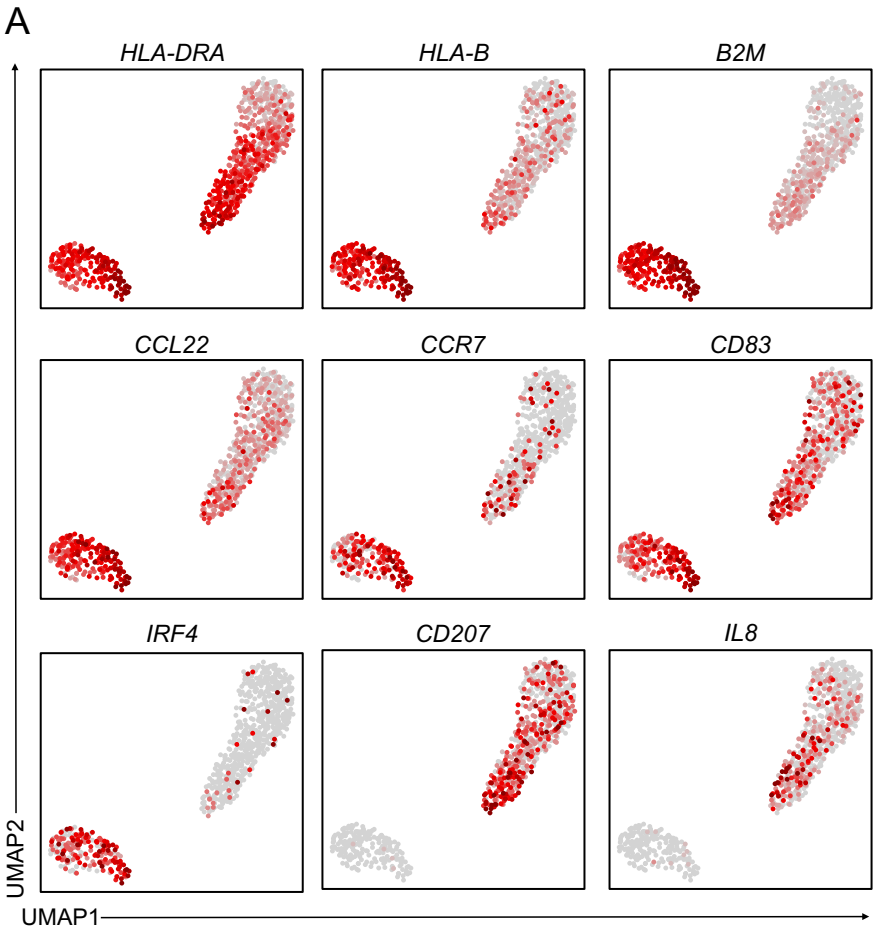

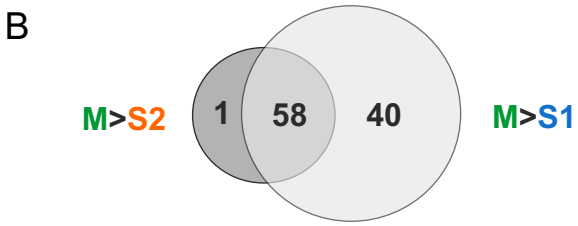

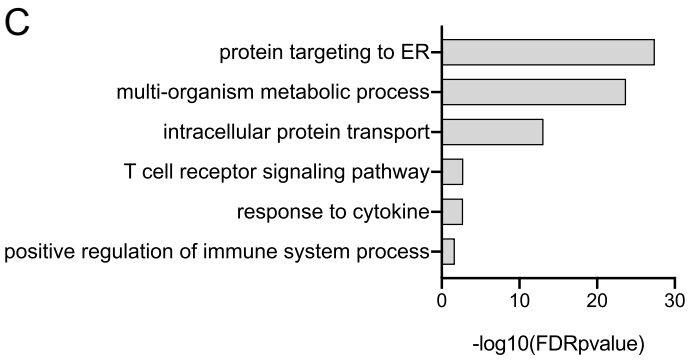

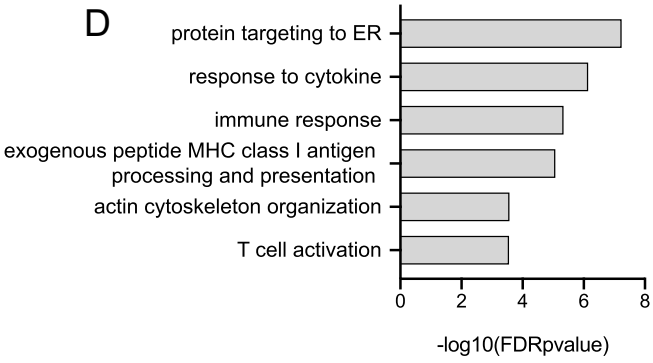

Supplementary Figure 5

A